

TUNNELING MAGNETORESISTANCE (TMR) ON Fe-Al₂O₃ NANO GRANULAR FILM GROWTH BY HELICON PLASMA SPUTTERING

S. Purwanto

Center For Technology of Nuclear Industry Materials
National Nuclear Energy Agency (BATAN)
Puspiptek Area, Serpong, Tangerang, Indonesia

ABSTRACT

TUNNELING MAGNETORESISTANCE (TMR) ON Fe-Al₂O₃ NANO GRANULAR FILM GROWTH BY HELICON PLASMA SPUTTERING. Fe-Al₂O₃ nanogranular thin film by helicon plasma sputtering with the variation of Fe content from 0.1 to 0.7 volume fraction have been prepared. The magnetic and magnetoresistance properties were investigated by a Vibrating Sample Magnetometer (VSM) and a Four Point Probe (FPP). The Rutherford BackScattering (RBS) was performed with the SIMNRA software. Conversion Electron Mossbauer Spectroscopy (CEMS) study was also performed to estimate the fraction of Fe and α -Fe₂O₃ in the granular film. The results suggested that the percolation concentration occurred at 0.55 Fe volume fractions, with the maximum Magnetoresistance (MR) ratio of 3%. The present MR ratio that was lower than the previous results may be related to the existence of α -Fe₂O₃ phase.

Keywords: Nanogranular thin film, Helicon Plasma Sputtering, Tunneling Magnetoresistance, Conversion Electron Mossbauer Spectroscopy, Rutherford Back Scattering(RBS)

INTRODUCTION

Recently research in Tunneling Magnetoresistance (TMR) has been growth rapidly. The TMR material has opened new perspective in the physics of magnetotransport and also provides many possibilities for further improvement of magnetoresistance devices like sensor, read head, MRAM etc. [1]. One kind of interest materials to exhibit TMR is a granular film consisting of nanometer sized magnetic metal like Fe embedded in insulators which caused by spin dependent tunneling between magnetic granules [2].

Different from Zhu et.al works[3], where they prepared Fe-Al₂O₃ film on well cleaned glass substrates by rf sputtering from a composite target consisting of at Fe plate placed on an Al₂O₃, the present research interest is aimed to do development of the TMR material by using Helicon Plasma Sputtering method [4]. The applied TMR materials are thin film of Fe-Al₂O₃ deposited on Silicon single crystal.

EXPERIMENTAL METHODS

Fe-Al₂O₃ thin films with the different content of Fe content from 0.1-0.7 volume fraction are deposited on Silicon single crystal by Helicon

plasma sputtering technique. We estimate the composition by controlling the alternating time exposure of the target during deposition without break the vacuum.

The basic pressure of the chamber was lower than 1×10^{-7} Torr and the target size is 50 mm in diameter. The substrate can be rotated during deposition to get uniform layer and the Argon gas pressure has to be maintained at 6.9×10^{-4} Torr. Deposition rate of materials are set at 0.6 Å/sec and 0.08 Å/sec for Fe and Al₂O₃ target, respectively. The X ray diffraction (XRD) patterns of the samples were measured to investigate crystalline structure and to estimate the grain size. The magnetic properties were measured with Vibrating Sample Magnetometer (VSM) at room temperature. The magnetoresistance (MR) was obtained by four points probe method in plane field, with the maximum field of 15 kOe. Rutherford backscattering (RBS) measurements were carried out with 2.5 MeV He⁺ ions using a geometry of 170° to determine the atomic composition. The RBS was performed with the SIMNRA software [5]. Conversion Electron Moosbauer Spectroscopy (CEMS) study was also performed to estimate the fraction of Fe and α-Fe₂O₃ in the granular film.

RESULTS AND DISCUSSION

Crystalline Structure and Crystallite Size

Typical X ray diffraction patterns (XRD) for the Fe-Al₂O₃ granular film are shown in Figure 1 for various Fe volume fraction. With decreasing the Fe volume fraction, the peaks intensity became weakens and width broadens, an indication that the Fe crystallite size became smaller from 1.98 nm to 0.79 nm for Fe volume fraction 0.66 and 0.19 respectively. To determined the crystallite size, we analyze the Fe (110) peak with Gaussian profile and use the Scherrer formula as follows;

$$\text{Crystallite size } d = K \lambda / B \cos \theta \quad (1)$$

K is the shape factor of the average crystallite (expected shape factor is 0.9), λ is the wavelength (usually 1.54056 Å for Cu Kα), θ is the peak position in radian and B is half width of a given diffraction peak.

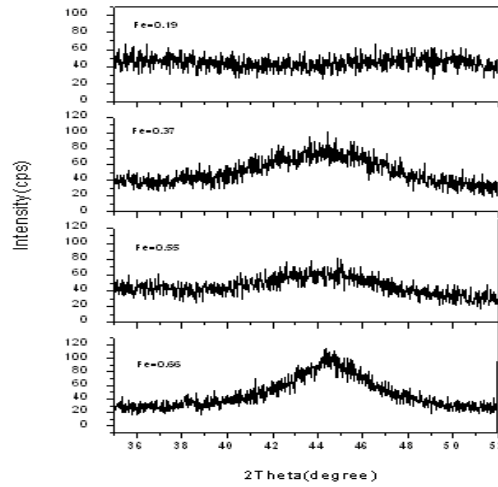


Figure 1. The peaks correspond to the Fe[110] as a function of Fe volume fraction in Fe-Al₂O₃ granular film and its crystallite size d.

Rutherford Backscattering (RBS) and CEMS Measurement

The Rutherford Backscattering (RBS) have been performed to determine the atomic composition in of the Fe-Al₂O₃ granular film. Figure 2 shows one example of RBS pattern for sample no 3 for deposition time of 120 minutes compared to sample no 13. Then, the RBS pattern was fitting with SIMNRA software to estimate the composition of the film as summarized in Table 1.

Table 1. Composition of Fe-Al₂O₃ granular film determined by RBS and fraction of α -Fe and α -Fe₂O₃ by CEMS.

Sample No	Fe content		
	Vol. fraction	α -Fe (%)	α -Fe ₂ O ₃ (%)
3	0.6614	95	5
5	0.5485	75	25
8	0.3652	56	44
13	0.1949	44	56
14	0.1330	not calc.	not calc.

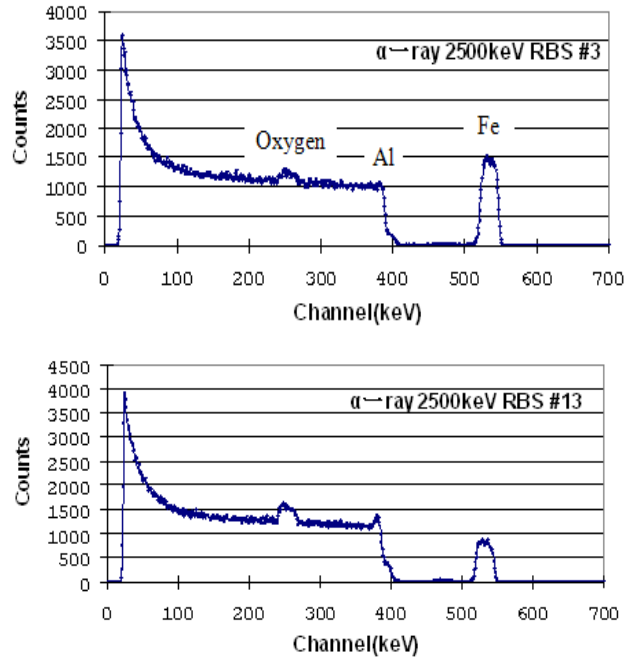


Figure 2. RBS pattern for Fe-Al₂O₃ sample no 3 with Fe volume fraction 0.66. and sample no 13 with Fe volume fraction 0.19,at room temperature.

Magnetic Properties

Magnetization curves of the Fe-Al₂O₃ granular film were showed in Figure 3, as a function of Fe volume fraction.

As showed in the figure, for the Fe volume fraction of 0.66 with granular diameter of $d = 1.98$ nm, the strong ferromagnetic coupling still coexist with paramagnetic component. Saturation magnetization M_s was only 600 emu/cc, small enough compare to the fraction saturation value of α -Fe ($M_s = 0.66 \cdot 1700$ emu/cc = 1122 emu/cc). This fact suggests that there is another phase of magnetic component i.e α -Fe₂O₃ which has been confirm by RBS and CEMS measurement result as shown in Table 1. Based on the Conversion Electron Moosbauer Spectroscopy (CEMS) spectra, there are two magnetic phase i.e α -Fe and α -Fe₂O₃ beside paramagnetic component. This situation also found for Fe-Al₂O₃ film grown by RF sputtering with different particle distribution [5]. Detail on CEMS study not presented here [7]. It is clear that the superparamagnetic behavior became appears while Fe volume fraction decreases.

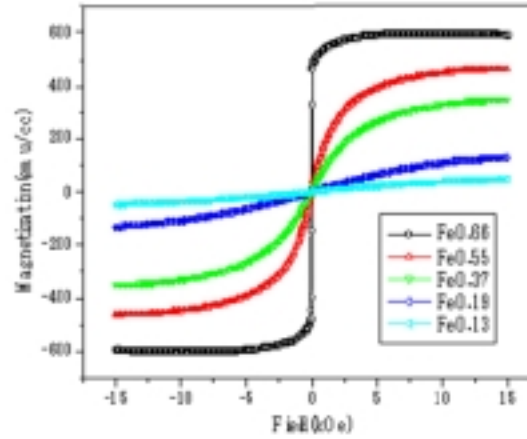


Figure 3. In plane magnetization curves for Fe-Al₂O₃ as a function of Fe volume fraction at RT.

Using the equation based on Langevin function for granular film by assuming the system have two particle size distributions, it can be written as follows;

$$M = M_s \sum w_i L(A_i H) \text{ for } i=1,2 \quad (2)$$

Where $L(x) = \coth(x) - 1/x$ is the Langevin function, and

$$A_i = (4\pi/3)r_i^3 M_s/k_B T, \text{ } i=1,2 \quad (3)$$

In equation (2), w_i ($i = 1,2$) is the weighing factor for the particle concentration with particle size of radius r_i ($i = 1,2$), respectively, where $\sum w_i = 1$. The quantity M_s is the spontaneous magnetization of the Fe particles to determined by the best fit, and k_B is the Boltzmann constant.

Figure 4 shows the fitting result for sample no 5 with deposite time of 120 minutes. In the fitting we observed that w_1 is 0.45 and w_2 is 0.55 with granular size $r_1 = 1.1$ nm and $r_2 = 1.7$ nm, an indication the occurring of small and large granular, respectively. The complete M-H curve fitting results was summarized in Table 2.

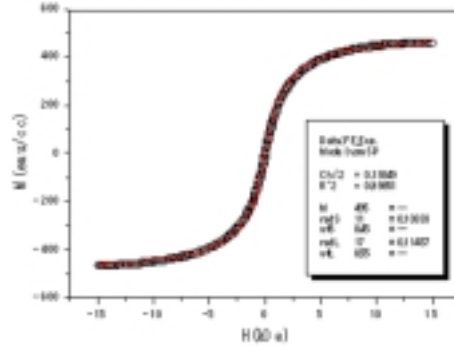


Figure 4. Measured magnetization hysteresis data versus field at RT for sample no 5 with deposit time of 120 minutes .Solid line is the fitted curve using equation (1) with w_1 or $w_s= 0.45$ and w_2 or $w_L= 0.55$ with granular radius $r_1= 11$ A and $r_2= 17$ A, respectively.

Table 2. M-H curve fitting results for Fe-Al₂O₃ granular film.

Sample no	Fe vol. fraction	w_1	r_1 (nm)	w_2	r_2 (nm)	M_s (emu/cc)
3	0.66	0.15	3.0	0.85	3.5	610
5	0.55	0.45	1.1	0.55	1.7	495
8	0.37	0.365	0.99	0.635	1.3	382.3
13	0.19	0.35	0.8	0.65	0.86	180
14	0.13	0.30	0.79	0.70	0.82	65

Magneto-resistance and Resistivity

In Ferromagnetic (F) - Insulator (I) films [7], the Tunneling magneto-resistance ratio can be expressed here under :

$$\Delta\rho/\rho = P^2m^2/(1+P^2m^2), \quad (4)$$

where P is the spin polarization of the granules. We take P for Fe is 0.44 [9] and $m = M/M_s$ the magnetization normalized by the saturation magnetization M_s . The $m = 0$ ($m = 1$) corresponds to the randomly (fully) oriented magnetic moments of the granules in the zero (high) magnetic field. As indicated by N.Wisher [10] and provided by Wang et.al[11], the spin polarization in the Ferromagnetic-Insulator film (here Fe-Al₂O₃) is dependent not only to the property of ferromagnetic metals but also to the matrix characteristic of Al₂O₃, such as the structural and electronic properties of the entire films including the matrix. Then we adopt the modified Eq.(4), as Wang et.al proposed, as follows;

$$\Delta\rho/\rho = x_1k_1P^2m_1^2/(1+P^2m_1^2) + x_2k_2P^2m_2^2/(1+P^2m_2^2) \quad (5)$$

here if $k_2 > k_1$, single domain granular play a key role in TMR, otherwise, superparamagnetic granular does in TMR. x_1 and x_2 are the fraction of superparamagnetic granular and single domain granular occupied whole ferromagnetic granular, respectively. We introduce parameter k_1 and k_2 being the weight factor of superparamagnetic granular and single domain granular. We analysed the magnetoresistance curve with the Eq.(5) to get all the parameter like k_1, k_2, x_1, x_2, r_1 and large granular radius- r_2 , and summarized in Table 3.

Table 3. Result of Magnetoresistance Curve Fitting by Eq.(5).

Sample no	Fe vol. fraction	x_1	r_1 (nm)	x_2	r_2 (nm)	k_1	k_2
3	0.66	0.44	0.88	0.56	1.72	5.47	6.70
5	0.55	0.40	1.14	0.60	1.46	9	28
8	0.37	0.355	1.05	0.645	1.27	15	20
13	0.19	0.40	0.77	0.60	0.80	15.8	20
14	0.13		0.80		0.82		

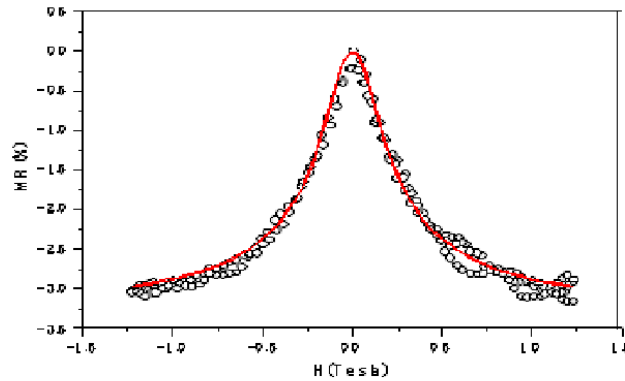


Figure 5. Magnetoresistance curve fitted by equation 5 for Fe- Al_2O_3 granular film sample no 5.

The summarized of MR measurement and resistivity of Fe- Al_2O_3 granular was showed in Figure 6.

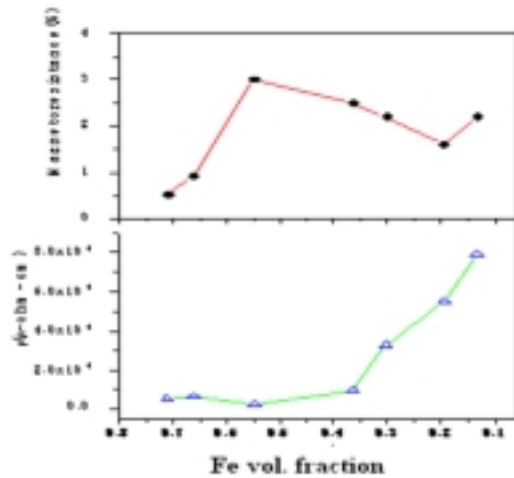


Figure 6. Resistivity and Magnetoresistance ratio of Fe-Al₂O₃ granular film as a function of Fe volume fraction.

Magnetoresistance Curve Evolution

Figure 7, shows the evolution change from negative magnetoresistance into positive magnetoresistance (PMR) due to the ratio between α -Fe and α -Fe₂O₃ as found by RBS and CEMS and tabulated in Table 1. The sample no 3, 5 and 8 have negative magnetoresistance with MR ratio -0.9, -3.0, -2.5%, respectively. In those samples the α -Fe content is greater compared to α -Fe₂O₃. While the anomalous from negative MR to positive MR was occur in sample no 13 with Fe volume fraction 0.19 and ratio between the α -Fe content is 44% compared to 56% for α -Fe₂O₃. We suggest that the mechanism charge transfer between Fe grain was depended on the existence of Fe₂O₃ barrier beside the Al₂O₃ matrix insulator. This situation also found in another system like (Fe₂O₃)_{1-x}(Fe₃O₄)_x ferrites as reported by A.C Sun et.al [13]. The changes of MR curve from negative to positive MR were also reported by Hsu et.al [14]. They found such kind anomalous in Ag_x(Fe₃O₄)_{1-x} for $x < 0.02$. Different view was also reported by Teixeira et.al [14] for Fe-Al₂O₃ sample which prepared by dual electron beam sputtering. At 40 K for high bias voltage above 2.5V, they found inversion of MR curve. In this situation this phenomenon was related to the inversion of spin polarization as propose by Sharma et.al [16] and also observed by De Teresa et.al [17] for tunneling junction.

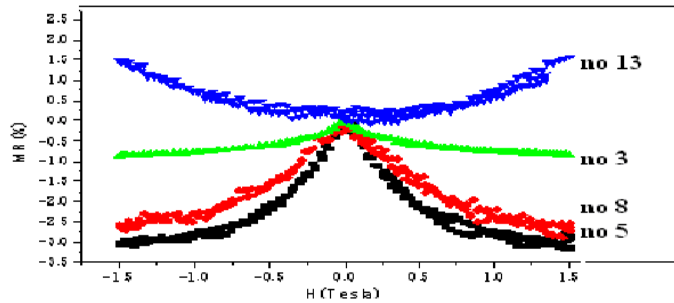


Figure 7. Magnetoresistance curve evolution in Fe-Al₂O₃ granular film for sample no 3,5,8 and 13 with Fe volume fraction of 0.66,0.55,0.37 and 0.19 respectively.

CONCLUSION

We have developed a nanogranular film Fe-Al₂O₃ that exhibits a tunneling magnetoresistance by Helicon Plasma Sputtering method. We could control the composition by means of alternating exposure time of the target without breaking the vacuum. The percolation concentration was occur at 0.55 Fe volume fraction, with maximum MR ratio 3%. The MR ratio was lower than the results of Zhu et.al (4.5% at percolation concentration) which can be related to the existence of Fe₂O₃ phase.

ACKNOWLEDGEMENT

This project was financially supported by the Budget for Scientist Exchange Program in Nuclear Energy Research of AIST and Nuclear Research of the Ministry of Education, Culture, Sports, Science and Technology- JAPAN, fiscal year 2004-2005.

REFERENCES

1. S.S. PARKIN., *Spin Dependent Transport in Magnetic Nanostructures*, Taylor & Francis, New York, **3** (5) (2002).
2. S. MITANI, H. FUJIMORI and S. OHNUMA, *J. of Magn. And Magn. Matter*, **165**, 141 (1997).
3. T. ZHU and Y.J. WANG, *Phys. Rev. B*, **60**, 11918 (1999).
4. M. KOIKE, M. CHIKAWI, ISAO H. SUZUKI and N. KOBAYASHI, *Rev. Sci. Instrum.*, **66** (2) 2141 (1995).
5. ZIGGLER , SIMNRA software code.

6. A. ABELIEMU, H. WAKABAYASHI, S. MATSUZAWA, Y. NAKANISHI, T. TORIYAMA and I. SAKAMOTO, *Phys. Stat. Sol. (c)*, **1** (12) 3315 (2004).
7. T. TORIYAMA , private communication.
8. J. INOUE and S. MAEKAWA, *Phys. Rev.B*, **53**, R11927 (1996).
9. P.M. TEDROW and R. MESERVEV, *Phys. Rev.*, **B7**, 318 (1973).
10. N. WISHER, *J. of Magn. and Magn. Matter*, **159**, 119 (1996).
11. C. WANG, Z. GUO, Y. RONG, and T.Y. HSU, *Phys. Lett. A*, **329**, 236 (2004).
12. S. HONDA, T. OKADA, M. NAWATE, and M. TOKUMOTO, *Phys. Rev. B.*, **56** (22) 14566 (1997).
13. A.C SUN, *J. of Magn. and Magn. Matter.*, **272-76**, 1776 (2004).
14. J.H. HSU, S.Y. CHEN, W.M. CHANG and C.R. CHANG, *J. of Magn. and Magn. Matter*, **272-76**, 1772 (2004).
15. S.R. TEIXIARA , M.A.S. BOFF, W.H. FLORES, J.E. SCHMIDT and M.C.M. ALVES, *J. of Magn. and Magn. Matter*, **233**, 96 (2004).
16. M. SHARMA, S.X. WANG and J.H. NICKEL, *Phys. Rev. Lett.*, **82**, 616 (1999).
17. J.M. De TERESA, A. BARTHELEMY, A. FERT, J.P. COUNTOUR, R. LYONNET, F. MONTAIGNE, P. SENEOR and A. VAURES, *Phys. Rev. Lett.*, **82**, 4288 (1999).